# Interfacing Methods for Combined Stability and Electro-magnetic Transient Simulations applied to VSC-HVDC

Arjen A. van der Meer, *Graduate Student Member, IEEE,* Ralph L. Hendriks, *Graduate Student Member, IEEE,* Madeleine Gibescu, *Member, IEEE* and Wil L. Kling, *Member, IEEE*

***Abstract*—This paper deals with the inclusion of voltage sourced converters (VSC) into power system stability assessment tools by interfacing a stability-type simulation with a more detailed electro-magnetic transient (EMT) simulation method. In this way, the influence of VSCs on ac systems, caused by the nonlinear behavior of these converters, can be analyzed accurately without the constraint of simulating the entire network in detail. A Matlab-based simulation framework is introduced and several aspects of combining these two types of simulations are experimented with.**

**The effectiveness of the described interfacing technique is explored on a test network. This is done by comparing the numerical performance of the proposed hybrid simulation method with a full EMT simulation, which is performed with PSS®NETOMAC. It turns out that particularly the (fast) controllers of VSCs are sensitive to the setup of the proposed interface. Moreover, the order in which the two types of simulations are solved in time influences the way dynamics of VSCs are reflected in the ac system. The paper highlights key parameters that determine the accuracy of the interface and concludes with suggestions to further improve the combined simulation concept.**

***Index Terms*—hybrid power system simulation, interfacing methods, VSC-HVdc.**

## I. INTRODUCTION

RECENT developments in power electronics have opened up new possibilities for the large-scale deployment of voltage sourced converters (VSC) for high power applications. Generators fed by renewable sources in remote locations, most notably wind-powered, may often be interfaced to the grid by VSCs. On transmission level the application of high-voltage dc (HVdc) transmission based on VSCs is becoming a mainstream technology. This offers interesting new options for future network expansion. In Western Europe, for instance, it is considered to expand the power system by VSC-HVdc links to integrate large amounts of offshore wind power, which may eventually lead to the establishment of transnational offshore grids based on dc technology.

This research is financially supported by Agentschap NL, an agency of the Dutch Ministry of Economic Affairs, under the project North Sea Transnational Grid (NSTG). NSTG is a joint project of Delft University of Technology and the Energy Research Centre of the Netherlands.

A. A. van der Meer, R. L. Hendriks, and M. Gibescu are with the Electrical Sustainable Energy Department, Faculty of Electrical Engineering, Mathematics, and Computer Science, Delft University of Technology, 2628 CD, Delft, the Netherlands (e-mail: A.A.vanderMeer@tudelft.nl, R.L.Hendriks@tudelft.nl, M.Gibescu@tudelft.nl)

W. L. Kling is with the Electrical Energy Systems Department, Faculty of Electrical Engineering, Eindhoven University of technology, 5600 MB, Eindhoven, the Netherlands (e-mail:W.L.Kling@tue.nl)

Future networks must be analyzed in detail in planning studies performed today. An important part of such studies is transient stability simulation. These simulations are based on a well-established framework of assumptions and modeling simplifications that have developed over the past decades. Transient stability simulations are mainly concerned with the dynamics of synchronous generators and their control systems. These phenomena have a typical bandwidth of 1–10 Hz. This allows the transmission network to be modeled in a quasi steady-state fashion by stationary complex phasors.

The incorporation of power electronic interfaces, particularly VSCs, into stability simulations is a major challenge. VSC dynamics are several orders of magnitude faster than machine dynamics. In itself these fast dynamics are not very important to transient stability, which would plea for the use of idealized VSC models. Unfortunately, electrical transients induced by power electronics might trigger control features or protective circuits that can have a significant influence on ac machine dynamics and hence need to be taken into account when assessing system stability. Most transient stability analysis tools do not offer a structural solution to this problem, and each type of power electronics equipment model requires careful individual consideration. Especially when the dc networks extend beyond point-to-point links, i.e. with three or more terminals to the ac network, current simulation methods are insufficient.

Accurate dynamic simulation of power electronics can be performed by electro-magnetic transient (EMT)-type solvers. In this type of simulation electrical network quantities are modeled by differential equations. Hence, a much smaller time step size is required than for stability-type simulations, and the models are computationally complex. Generally speaking, EMT-type simulations are not suitable for large networks.

This paper deals with the inclusion of VSC-based grid interfaces into stability-type simulators by hybrid methods. With such methods those parts of the system having fast dynamics, i.e. the VSCs and dc networks, are covered by EMT-type simulations. These are subsequently coupled to the stability type simulation, which is used for the rest of the network. These methods allow existing stability models to be used, and offer the advantage of including power electronics in a unified manner with high accuracy. Hybrid simulations offer notable improvement in accuracy compared to stability-type simulations and may provide lower execution times as compared to EMT-type simulations.

In this paper a simulation framework is presented, developed in Matlab, which includes both stability- and EMT-type simulation methods. This framework can be used for experimenting with different interfacing methods between the two types of simulation. The paper starts with a description of the two types of simulations. The stability simulation part is based on a partitioned-solution approach by a predictor-corrector method. The EMT part is implemented according to the nodal analysis method, employing the trapezoidal rule for integration. The used VSC model and its inclusion in the presented solution scheme is briefly elaborated upon. Then, several important aspects of the interface between the two types of simulation are discussed and parameters that establish the numerical performance are highlighted. This is done by looking at the simulation accuracy when performing simulations on a test network. In this respect, comparison with a full EMT simulation is made. The paper ends with conclusions and directions for further research.

## II. Hybrid simulation framework

The hybrid simulation environment has been developed in Matlab. It contains three main parts. The stability type simulation, which employs the largest time step size, is the main simulation environment, and the largest part of the network is expected to be simulated by this method. The EMT-type simulation is included by an inner integration loop and is expected to contain the part of the network that needs a higher level of detail, such as dc networks and VSCs. The interface couples both simulations by representing each submodel into the other by means of equivalent current and voltage sources.

### *A. Stability type simulation*

Grid integration studies usually include the assessment of system stability. Although stability covers a wide range of definitions [1], here we are mainly concerned with transient stability, i.e. the ability of the ac system to remain in synchronism during electromechanical oscillations. As the frequency of these oscillations is relatively low, time domain simulation can be performed with a well-established set of simplifying assumptions [2]. Among these are, most prominently, the simulation of network quantities by stationary complex phasors, using single line equivalents (for symmetric faults), and a simplified representation of synchronous generators and governing systems.

Stability-type simulations concern the solution of a set of differential-algebraic equations (DAE), given by

$$\dot{\boldsymbol{x}} = f(\boldsymbol{x},\boldsymbol{y}) \tag{1}$$

$$\boldsymbol{0} = g(\boldsymbol{x},\boldsymbol{y}) \tag{2}$$

in which $\boldsymbol{x}$ is a vector containing state variables and $\boldsymbol{y}$ is the vector of algebraic variables. Equation (1) represents the dynamic behavior of generators, exciters, governors, sometimes including dynamic loads, whereas (2) represents the algebraic set of equations, consisting of the network solution, static load models, and algebraic controller equations. By solving (1) and (2) each time step, the dynamic response of the system is obtained. Generally, two methods to solve (1) and (2) are commonly used. Partitioned explicit (PE) methods calculate the two sets of equations sequentially by solving (1) by any explicit numerical integration method. Subsequently, the set of algebraic equations is solved. Simultaneous implicit (SI) methods discretize the set of differential equations by applying implicit numerical integration methods. These equations are then solved together with the algebraic equations [3]. PE methods have the advantage of programming flexibility, but a relatively large interface error between the differential and the algebraic part of the solution. This error does not exist for SI methods, as (1) and (2) are solved iteratively. This allows to simulate using a larger time step size without compromising simulation accuracy. In this study the PE method is chosen for its particular programming merits.

The employed PE method uses explicit numerical integration methods to solve (1) over a discretized time interval. In this case a single-step predictor-corrector method is used to solve the set of DAEs at each time step. This method has the benefit of reducing the interface error between the differential and algebraic variables [4]. The state variables at time $t_n$, $\boldsymbol{x}_p^{t_n}$, are approximated by a forward Euler predictor

$$\boldsymbol{x}_p^{t_n} = \boldsymbol{x}^{t_{n-1}} + hf\left(\boldsymbol{x}^{t_{n-1}},\boldsymbol{y}^{t_n^-}\right) = \boldsymbol{x}^{t_{n-1}} + h\dot{\boldsymbol{x}}_p^{t_n} \tag{3}$$

with $h$ the time step size, which is kept fixed throughout the simulation, and is typically in the order 1–20 ms, depending on the model complexity. If a discontinuity occurs at $t_n$, for instance a short-circuit, line tripping, or load (dis)connection, $0 = g(\boldsymbol{x}^{t_{n-1}},\boldsymbol{y}^{t_n^-})$ must be solved to obtain accurate starting values for (3). If no network changes take place at $t_n$, $\boldsymbol{y}^{t_{n-1}}$ can be used as a starting point. $\boldsymbol{y}_p^{t_n}$ may be obtained by either extrapolation from previous values or by solving (2). The predicted value for $\boldsymbol{x}^{t_n}$ is now corrected by a trapezoidal corrector according to

$$\boldsymbol{x}_c^{t_n} = \boldsymbol{x}^{t_{n-1}} + \frac{h}{2}\left[\dot{\boldsymbol{x}}_p^{t_n} + f\left(\boldsymbol{x}_p^{t_n},\boldsymbol{y}_p^{t_n}\right)\right] \tag{4}$$

By using $\boldsymbol{x}_c^{t_n}$ as a new prediction and iterating until convergence, the accuracy of (4) can be improved to acquire $\boldsymbol{x}^{t_n}$. Subsequently, (2) can be extrapolated or solved iteratively to obtain $\boldsymbol{y}^{t_n}$. The overall solution scheme is depicted in Fig. 1.

### *B. Electromagnetic Transient Simulation*

Studies for detailed analysis of power system behavior in the time domain usually focus on electro-magnetic oscillations ( because of switching and lightning phenomena ), power system harmonics, and the nonlinear behavior of devices such as power electronics converters. The assumptions used for stability-type simulations, most notably the simplified modeling of network elements, are no longer valid. The EMT part of the proposed simulation framework is particularly designed for simulation of VSCs and dc-networks and is based on the well-developed nodal analysis method [5], [6]. In this method, the network is represented by differential equations, which are discretized by integrator substitution using the trapezoidal rule.

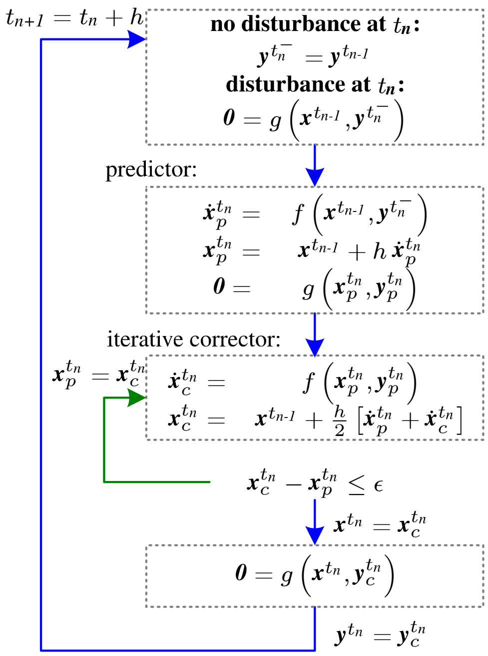


Fig. 1. Predictor-corrector solution scheme for the stability type simulation

*1) Branch representation:* The implementation of the nodal analysis method into the simulation framework is based on the one-port representation of branches depicted in Fig. 2. Each branch can be modeled by a branch current source $I_{inj}$ and / or a voltage source $E_{br}$, together with an equivalent resistance $R_{eq}$. On a network level, the branch voltages and currents are related from Kirchhoff's laws by

$$\boldsymbol{A}\boldsymbol{Y}_b\boldsymbol{v}_k = \boldsymbol{A}\left[\boldsymbol{Y}_b\boldsymbol{E}_{br} - \boldsymbol{I}_{inj}\right] \tag{5}$$

with $\boldsymbol{A}$ the reduced adjacency matrix, $\boldsymbol{Y}_b$ the branch admittance matrix, $\boldsymbol{v}_k$ the branch voltages, $\boldsymbol{E}_{br}$ the external voltage sources, and $\boldsymbol{I}_{inj}$ the modeled current injections. The branch voltages are related to the node voltages by

$$\boldsymbol{v}_k = \boldsymbol{A}^T\boldsymbol{v}_n \tag{6}$$

where $\boldsymbol{v}_n$ is the vector containing the node voltages. With substitution of (6) into (5), the nodal form is obtained

$$\boldsymbol{Y}_n\boldsymbol{v}_n = \boldsymbol{i}_n \tag{7}$$

where $\boldsymbol{Y}_n$ is the nodal admittance matrix and $\boldsymbol{i}_n$ the vector of nodal current injections.

*2) Numerical integrator substitution:* The differential equations for the network elements and the controllers are discretized by means of the trapezoidal rule of integration. This is a widely adopted method for calculating power system transients. It relies on the fact that for a predefined fixed time step size $h_{emt}$, the passive branch elements in $\boldsymbol{Y}_b$ are included by the relationship between currents and voltages for that particular time-step size. Furthermore, the history terms, which result from the implicit character of the trapezoidal rule, are included by current injections at $t_m$. For an inductor $L$ between node $p$ and $q$, for instance, the corresponding

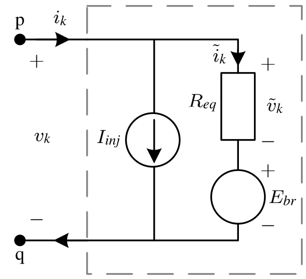


Fig. 2. Branch model used for the EMT-type simulation.

differential equation can be discretized by the trapezoidal rule, which relates the inductor current with the branch voltage by

$$\begin{aligned} i_{k,pq}^{t_m} &= i_{k,pq}^{t_{m-1}} + \frac{h_{emt}}{2L}\left(v_{k,pq}^{t_{m-1}} + v_{k,pq}^{t_m}\right) \\ &= i_{hist}^{t_{m-1}} + \frac{1}{R_{eq}}\left(v_{k,pq}^{t_m}\right) \end{aligned} \tag{8}$$

where $i_{k,pq}$ and $v_{k,pq}$ are the branch current voltage respectively. The parts of (8) that depend on continuous and algebraic variables calculated during the previous time step(s) are often referred to as the history terms. The branch current injection $I_{inj}$ at $t_m$ therefore consists of both history terms (from $t_{m-1}$) and modeled (external) current injections (at $t_m$ ). Handling discontinuities such as faults, branch switching, and inclusion of power electronic valves, requires careful considerations regarding recalculation of the history terms by extrapolation [7], [8]. In this study, discontinuities are foreseen to occur in the ac network only and are therefore handled by the stability-type simulation.

Controllers can conveniently be included into the described modeling approach by equivalent voltage or current sources. The concerned control modules are discretized in the same way as the network elements by transforming the Laplace operator $s$ to the $z$-domain by $\frac{2}{h_{emt}}\frac{1-z^{-1}}{1+z^{-1}}$ according to the bilinear transform. In order to reduce the influence of algebraic loops and to reduce numerical oscillations, controller outputs are interfaced with the network part of the EMT simulation by a delay of $h_{emt}$.

Network voltages are calculated by solving (7) for $\boldsymbol{v}_n$ each time step. The known quantities are the controlled sources and the history terms, related to each other by (5). The overall solution scheme is shown in Fig. 3.

## C. Representation of VSCs

Future HVdc networks, particularly offshore, will be based to a large extent on VSC technology. To accurately assess the behavior of these converters, VSCs will be represented in the EMT part of the simulation framework. In this paper the VSC is modeled by an averaged model, which uses the active power balance to couple the ac and dc circuits [9], [10]. The general structure of the model is shown in Fig. 4 and consists of a part that is included into the network solution (VSC interface) and a control part that is solved afterwards. The dc terminals of the converter are represented by a current injection ($i_{dc}$) between the negative and positive poles whereas the ac terminal is

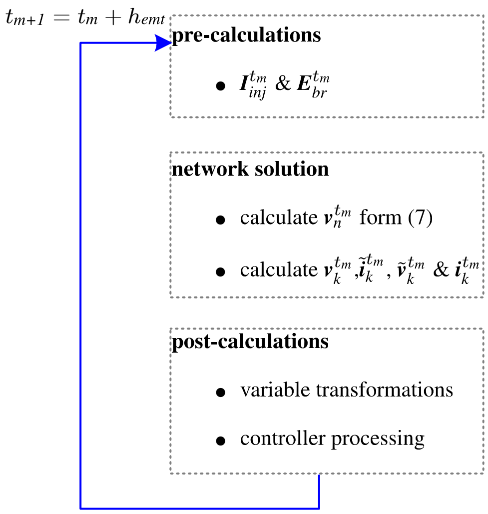


Fig. 3. Numerical solution scheme for the EMT part of the hybrid simulation framework.

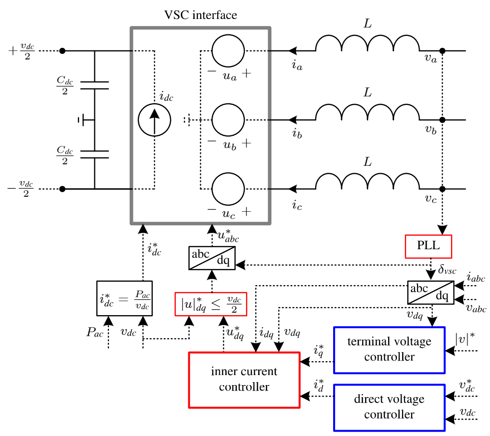


Fig. 4. Control scheme of the VSC model used in the EMT-type simulation.

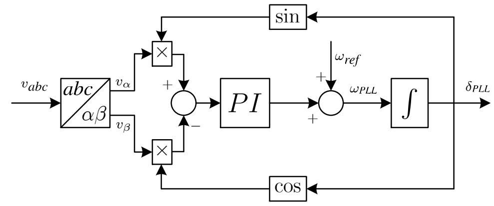


Fig. 5. $d$–$q$–$z$ type phase-locked loop used in the vector control scheme of the employed VSC model.

modeled by a three-phase voltage source ($u_{abc}$). This source conveys the output of the cascaded control structure, which is based on well-known vector control methods.

A key parameter regarding the performance of vector-controlled VSCs is the implementation of a phase-locked loop (PLL). This controller synchronizes the VSC control scheme with the terminal voltage by continuously adjusting the phase angle of an internal oscillator. When phase locked, the PLL allows independent control of active and reactive power. In this paper the $d$–$q$–$z$ type PLL is employed as shown in Fig. 12 [11]. A PI controller with a typical settling time of one fundamental frequency period controls the error signal, which is basically the angle between the space vector of the terminal voltage, $v_\alpha + \mathrm{j}v_\beta$, and the $d$–$q$ reference frame of the vector control scheme. If no control error exists, then $v_d = |v|$ and $v_q = 0$.

## III. Interfacing techniques

Hybrid simulators were first proposed and built in the 1980s by including a detailed model of a classical HVdc link into a stability-type simulation [12]. In [13], this approach was extended by investigating the influence of the network size of the system simulated by EMT. A different approach was introduced in [14]: a transition from detailed to quasi-steady state representation was implemented shortly (500 ms) after the disturbance, which introduced a significant improvement in execution times. Currently, the *IEEE task force on interfacing techniques for simulation tools* elaborates on the coupling of several power system simulation tools to each other, among which EMT and stability-type simulators [15]. In [16], [17], frequency-adaptive power system modeling was introduced, in which network quantities are represented in both EMT and stability at the same time, without actually defining interface locations. This method is most suitable when multi-time scale models for all connected devices are available. This may be a limitation for large networks and therefore, the hybrid simulation method is adopted here and extended to VSC-HVdc.

As stability-type and EMT-type simulations inherently differ in how — and in what level of detail — network quantities are calculated, both environments should be coupled. This coupling entails the representation of each network section into the other simulation environment, the transformation of network quantities, and the inclusion of the interface into the overall solution scheme.

### A. Network arrangement around the interface location

The major part of the ac system is simulated by a stability type simulation. At or around the connection nodes of VSCs, the network is modeled by the EMT-type simulation. The stability part can be represented into the EMT part in several manners, ranging from simple voltage sources to frequency-dependent equivalents [18]. Here, one straightforward method will be employed and its numerical implementation is studied.

Around the interface location, the ac system is represented in EMT by a Thévenin equivalent source, as shown in Fig. 6. Because all connected devices in the stability simulation are modeled by current injections, the subsystem simulated by EMT is represented into the stability part by a current injection as well. $Z^{th}$ is calculated at $t = 0$ s and is kept fixed for the entire simulation run. $\underline{E}_{th}$ can be calculated at the start of each stability simulation time step by

$$\underline{E}_{th} = \underline{V}_{int} + \underline{I}_{th} Z^{th} = E_{th} e^{\mathrm{j}\theta_{th}} \tag{9}$$

where $\underline{V}_{int}$ is the voltage phasor at the interface node at $t = t_n^-$, calculated in the stability-type simulation. For inclusion into the EMT-type simulator, $\underline{E}_{th}$ is transformed to a balanced set of three phase line-ground instantaneous voltages by

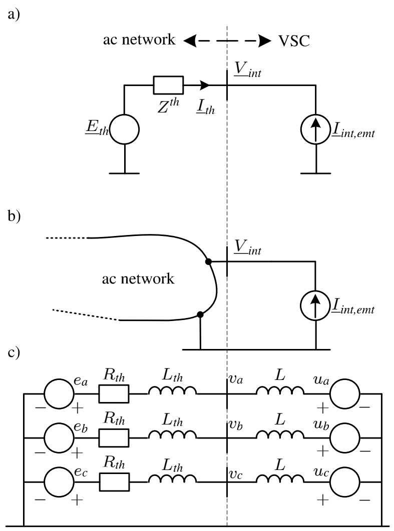


Fig. 6. a) Network arrangement around interface node. b) Interface representation in stability part. c) Interface representation in EMT part.

$$\begin{cases} e_a^{t_m} = \frac{\sqrt{2}}{\sqrt{3}} E_{th}^{t_{n\text{-}1}} \cos\left(\delta_{ref} + (t_m - t_{n\text{-}1})\omega_{ref} + \theta_{th}\right) \\ e_b^{t_m} = \frac{\sqrt{2}}{\sqrt{3}} E_{th}^{t_{n\text{-}1}} \cos\left(\delta_{ref} + (t_m - t_{n\text{-}1})\omega_{ref} + \theta_{th} - \frac{2\pi}{3}\right) \\ e_c^{t_m} = \frac{\sqrt{2}}{\sqrt{3}} E_{th}^{t_{n\text{-}1}} \cos\left(\delta_{ref} + (t_m - t_{n\text{-}1})\omega_{ref} + \theta_{th} + \frac{2\pi}{3}\right) \end{cases} \tag{10}$$

where

$$\delta_{ref} = \int_{t_0}^{t_{n\text{-}1}} \omega_{ref} \mathrm{d}t \tag{11}$$

with $\omega_{ref}$ the ac network fundamental frequency. It is assumed that the time step size of the stability-type simulation is the largest, i.e. $h > h_{emt}$. AC network quantities ( e.g. voltages, currents, power ) are hence available only after each large time-step $h$. Therefore, in between $t_{n\text{-}1}$ and $t_n$ the network quantities must be kept fixed or estimated. For instance, $\omega_{ref}$ is fixed when the reference node is modeled as a fixed-frequency voltage source and may vary in case it is represented by a slack generator. This may introduce an error in (10), particularly during and after disturbances.

Representing the Thévenin source by a variable-frequency voltage source may resolve this issue. As a first estimate, it is assumed that between $t_{n\text{-}1}$ and $t_n$ the mechanical torque and electro-magnetic counter torque of the synchronous generators in the connected network remain constant, and as a result the frequency may change linearly during this period. During the EMT simulation run, the system frequency $\omega_{ref}$ is approximated by

$$\frac{\mathrm{d}\omega_{ref}}{\mathrm{d}t} = \frac{\sum_{p=1}^{n} T_m^p - T_e^p}{2H_{eq}} \tag{12}$$

with $n$ the number of generators inside the connected ac system, $T_e^p$ and $T_m^p$ the electro-magnetic and mechanical torques of generator $p$ respectively, and $H_{eq}$ the equivalent inertial time constant, calculated by

$$H_{eq} = \sum_{p=1}^{n} H_p \tag{13}$$

The parts of the ac network included in the EMT-type simulation, which are for this study the VSC terminals and their phase reactors, are represented in the stability-type simulation by current injections at the interface nodes. As a first estimate, the VSC ancillary filters are not included, and $\underline{I}_{int,emt}$ can be derived from the VSC terminal current directly. This requires a transformation from instantaneous waveforms to phasors, which can be achieved e.g. by Fourier methods. Here, a non-recursive least-square error curve fitting method is used to obtain the fundamental frequency values of the waveforms [19]. At $t_n$, $\underline{I}_{int,emt}$ is defined as the positive sequence value of

$$\underline{I}_{int,012}^{t_n} = \frac{1}{\sqrt{2}} \boldsymbol{S}^{-1} \underline{I}_{abc} e^{-\mathrm{j}\delta_{ref}} \tag{14}$$

for $N = h/h_{emt}$ sampled values of $i_{abc}$, where

$$\boldsymbol{S}^{-1} = \frac{1}{3} \begin{bmatrix} 1 & 1 & 1 \\ 1 & e^{\frac{2\mathrm{j}\pi}{3}} & e^{\frac{4\mathrm{j}\pi}{3}} \\ 1 & e^{\frac{4\mathrm{j}\pi}{3}} & e^{\frac{2\mathrm{j}\pi}{3}} \end{bmatrix} \tag{15}$$

and $\underline{I}_{abc}$ is a phasor rotating counterclockwise with respect to a stationary reference frame with frequency $\omega_{ref}$, and can be calculated by

$$\underline{I}_{abc} = -\sum_{l=0}^{N-1} K_b^l i_{abc}^l + \mathrm{j} \sum_{l=0}^{N-1} K_a^l i_{abc}^l \tag{16}$$

in which

$$\begin{aligned} K_b^l &= \tfrac{1}{AC-B^2}\left[A \cos\left(l\,\omega_{ref}\,h_{emt}\right) - B \sin\left(l\,\omega_{ref}\,h_{emt}\right)\right] \\ K_a^l &= \tfrac{1}{AC-B^2}\left[C \sin\left(l\,\omega_{ref}\,h_{emt}\right) - B \cos\left(l\,\omega_{ref}\,h_{emt}\right)\right] \end{aligned} \tag{17}$$

and

$$\begin{aligned} A &= \sum_{l=0}^{N-1} \sin^2\left(l\,\omega_{ref}\,h_{emt}\right) \\ B &= \sum_{l=0}^{N-1} \sin\left(l\,\omega_{ref}\,h_{emt}\right) \cos\left(l\,\omega_{ref}\,h_{emt}\right) \\ C &= \sum_{l=0}^{N-1} \cos^2\left(l\,\omega_{ref}\,h_{emt}\right) \end{aligned} \tag{18}$$

### *B. Integration of the interface into the numerical solution scheme*

The variables to be exchanged at or around the interface node in Fig. 6 are $\underline{E}_{th}$ and $\omega_{ref}$ from the stability-type simulation and the positive-sequence current injection $\underline{I}_{int,emt}$ from the EMT-type simulation. The order in which this interface is coupled with the numerical solution schemes of Fig. 1 and Fig. 3 may considerably influence simulation performance. In this work, the simulation is executed in a partitioned fashion (i.e. EMT and stability parts separately), and information is exchanged at predefined instants. Fig. 7 shows the overall

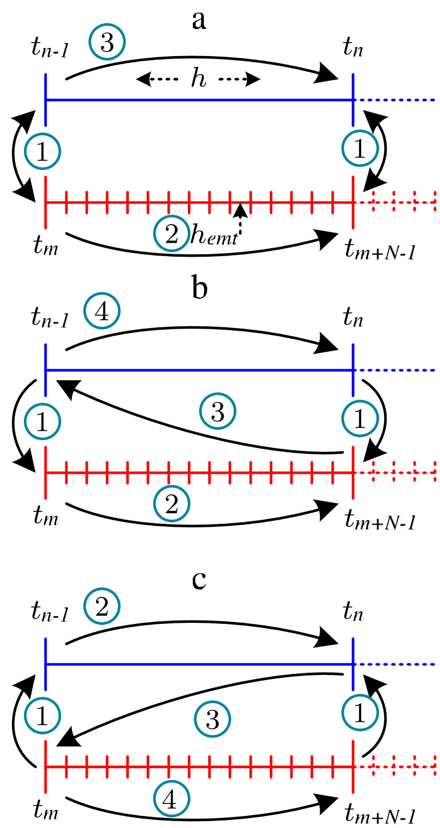


Fig. 7. Interfacing order in the hybrid simulation environment. blue: stability type simulation, red: EMT-type simulation. a) exchange after $h$ only b) the EMT part is calculated first c) the stability part is calculated first.

solution scheme of the hybrid simulation environment. Three fundamentally different arrangements can be distinguished. First, interfacing may take place after each calculation run of the stability part. In this case, solely information provided by the previous time step can be used in both simulations. Second, the EMT part of the simulation can be executed before the stability part. This offers the benefit of knowing detailed information about the behavior of VSCs and dc grids before the stability simulation is run. On the other hand, priority may also be given to the stability part. More sophisticated interfaces, such as interfacing both simulations at each corrector iteration, may improve the accuracy, but they are considered outside the scope of this paper.

## IV. Simulation Studies

The hybrid simulation framework is tested on the network arrangements shown in Fig. 8 and Fig. 9. Both networks contain three and five generators respectively. G1, G2, G4, and G5 are large generators which represent the equivalent dynamics of the adjacent power system areas and G3 is a smaller generator whose rotor angle is used to measure the accuracy of the hybrid simulation. G1 is the slack generator with the q-axis as reference. On the left side, two 330 MVA rated VSCs are connected to a common dc bus, each delivering the same amount of active power to the ac network. VSC 1 is modeled in the EMT part of the simulation framework using the provided model (see Fig. 4) whereas VSC 2 is included

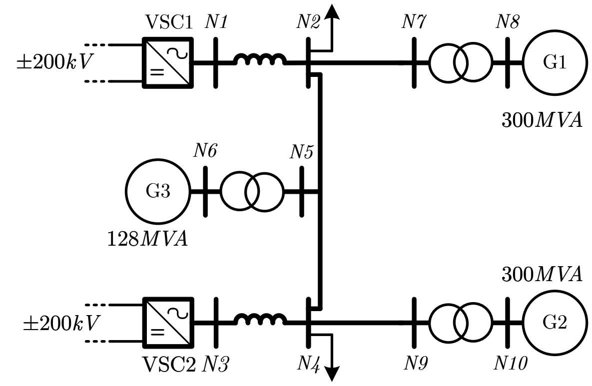


Fig. 8. Test network used for the simulation studies.

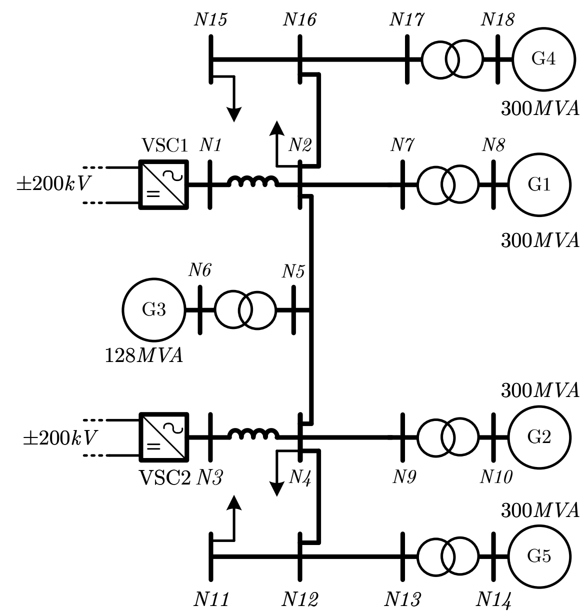


Fig. 9. Expanded network arrangement.

in the stability part while neglecting the dynamics of the fast inner controllers [20].

First, the hybrid simulation is tested on the network of Fig. 8. At $t = 0\,\mathrm{s}$, a Thévenin equivalent of the ac network is calculated (seen from the interface node N2) for the equivalent network representation in the EMT part. Throughout the simulation, $E_{th}$, $\delta_{ref}$, and $\theta_{th}$ are updated after each stability calculation step. At $t = 1\,\mathrm{s}$, a three-phase fault occurs at node N8 that is cleared after 100 ms. The simulation was executed for two different values of $h$, 1 ms and 10 ms, using the interfacing order shown in Fig. 7b. Furthermore, the accuracy of this particular case was compared with a full EMT simulation performed with PSS®NETOMAC. A time step size of 50 µs was chosen for all EMT simulations. The system response is shown in Fig. 10. First, it can be observed that the voltage profile at the interface node is similar for all simulations. However, the current injections, which are calculated according to the described curve fitting method, show a high sensitivity toward $h$. This can be explained by considering the current set points of VSC 1. As priority is given to the active part of the current (i.e. $i_d$), the reactive part

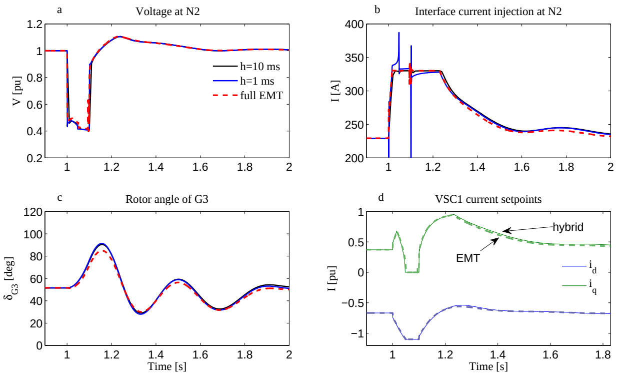


Fig. 10. System response of the network shown in Fig. 8 after a fault at node N8. a) Voltage amplitude at N2. b) amplitude of the $\underline{I}_{int,emt}$ in pu on a 1 MVA, 230 kV basis. c) Rotor angle of G3 d) direct and quadrature current set point of the outer controllers of the VSC.

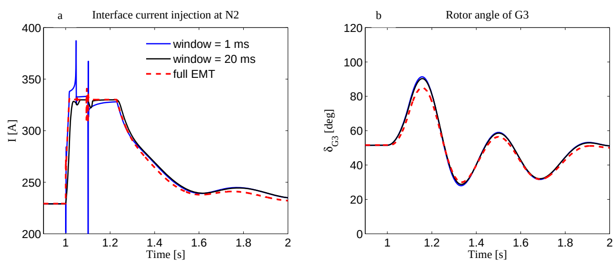


Fig. 11. System response for $h = 1$ ms following a fault at node N8 with increased sampling window size for curve fitting. a) Amplitude of $\underline{I}_{int,emt}$ in pu on a 1 MVA, 230 kV basis. b) Rotor angle of G3

must be curtailed in case the magnitude of the current set point exceeds the current limit of the converter. The inner current controller has a settling time in the order of 1–2 ms, which is (for $h = 1$ ms) equal to the length of the sampling window for curve fitting. This introduces inaccuracies with respect to the phase and amplitude of the waveforms on which the samples are fitted, most notably at instances when the current limiting starts or ends. This issue can be partly resolved by increasing the sampling window size to fit one fundamental frequency period, i.e. $N = \frac{2\pi}{h_{emt}\omega_{ref}}$. This is applied to the previous setup and the results are shown in Fig. 11. It can be seen that the peaks have now vanished for $h = 1$ ms as well. However, this is at the cost of a slightly slower response as the running rectangular sampling window is around 20 ms. This is most prominently issued after discontinuities in the VSC controller. This difficulty may be dealt with by using more sophisticated pre-filtering techniques.

Another slight difference between the EMT and hybrid simulations can be observed when the rotor angles of G3 are compared. This can be attributed to the fact that the coupling between (1) and (2) is solved by a slightly different numerical method. Moreover, machine stator transients are neglected in the presented stability simulation framework while these are taken into account in the transient section of PSS®NETOMAC.

The coupling between the stability part and the EMT part of the simulation is provided by the Thévenin equivalent source,

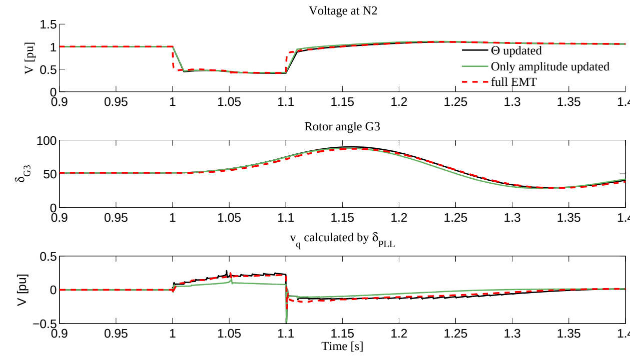


Fig. 12. Time-domain simulation for two particular implementations to update the Thévenin voltage source ($E_{th}$ alone versus both $E_{th}$ and $\theta_{th}$ )

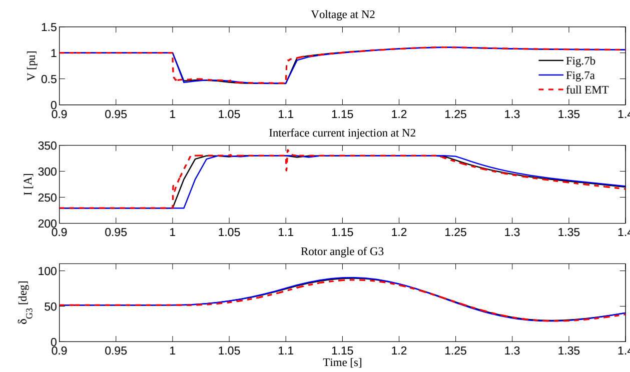


Fig. 13. Hybrid simulation executed using two different interfacing orders given in Fig. 7

which can be controlled and updated in several ways. Fig. 12 shows the system response for two particular methods to update this source. The black line shows the response to a fault if all variables in (10) are updated after each stability run, whereas the green line gives the response when all variables except $\theta_{th}$ are updated. It can be seen that updating both $\theta_{th}$ and $E_{th}$ gives a more accurate system response as compared to updating $E_{th}$ alone, despite the relatively high sensitivity of the PLL to the discontinuities caused by this. The response may be improved by smoothing out these sudden changes by including the changes in $\theta_{th}$ into the model of the dynamic equivalent, which now merely consists of the swing equation.

In order to show the effect of the interface data exchange order, the first simulation was also executed with the solution order of Fig. 7a. For $h = 10$ ms, the results are shown in Fig. 13. A slight difference between the two interfacing orders can be observed, which is related to the fact that the current provided by the VSC at $t = t_{n-1}$ is not injected into the stability part of the system until $t = t_n$. For normal operation, this error is considered acceptable. However, during discontinuities such as disturbances this delay may result in too optimistic frequency deviations and critical clearing times.

Until now, the network of Fig. 8 has been used for all simulations. Several methods have been tested and the effects on simulation accuracy has been addressed. It is however key to investigate how the discussed interfacing method performs

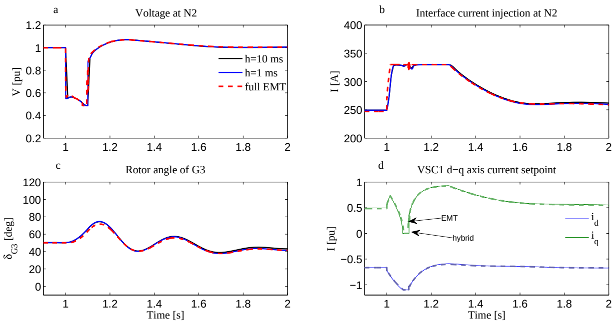


Fig. 14. System response of the network shown in Fig. 9 after a fault at node N8. a) Voltage amplitude at N2. b) amplitude of the $\underline{I}_{int,emt}$ in pu on a 1 MVA, 230 kV basis. c) Rotor angle of G3 d) direct and quadrature current set point of the outer controllers of the VSC.

in combination with a different network. Therefore, the discussed simulations have been repeated for the network shown in Fig. 9. In 14, it can be seen that although the network is almost twice as large as the network of Fig. 8, hardly any differences can be observed with respect to Fig. 11. This is in line with what could be expected: the share of VSC 1 with respect to the total installed generation capacity in the ac grid has been decreased. Consequently, negative (numerical) effects of the interface on the system response will be inferior to those issued in a relatively small network.

## V. Conclusion

At the transmission voltage level, a growing share of power electronics-based converters such as VSCs is expected in the coming decades, most prominently induced by the deployment of renewables. These converter-interfaced renewable plants show different dynamic behavior compared to traditional power plants, which must be taken into account in studies that focus on stability. For accurate representation of VSCs within these studies, combined simulation methods can be used.

This paper described a hybrid simulation framework particularly designed to include VSCs accurately into stability-type simulations. This has been achieved by including an averaged VSC model based on vector control in an EMT-type simulation. Subsequently, this simulation was interfaced with a stability-type simulation. This interface consists of three parts: an equivalent representation of the ac network in EMT, a method to capture waveforms into stationary complex phasors, and an appropriate numerical coupling and data exchange between the two simulations.

The described interfacing techniques were implemented and tested on two different network arrangements. It turned out that generally speaking, the hybrid simulation was accurate with respect to a full EMT-type simulation. It was shown that the accuracy of the VSC response considerably depends on the way in which updating the network quantities, i.e. phase angle, amplitude and frequency deviation are implemented into the Thévenin equivalent source. Based on the observations, it can be concluded that updating the amplitude of the Thévenin source without updating the phase angle is less accurate than updating both, despite a smoother response of the PLL.

The second notable feature of the presented interfacing techniques is that the method to capture stationary phasors from three-phase waveforms is only accurate when the considered sampling window is relatively large, because of the fast changes in the phase currents induced by the VSC's current controller. This is most prominent in the event of discontinuities ( e.g. when control limits are hit).

It has been shown that the order in which stability- and EMT-type simulations are numerically solved results in differences in the system response. The hybrid simulation results lie more closely to the full EMT simulation in case the EMT-part of the hybrid simulation is solved first during each calculation step. This difference can be of importance, particularly when the influence of VSCs on the connected power system is expected to be significant.

The presented simulations have given rise to new challenges with respect to representing VSCs (and hence dc networks) accurately into stability-type simulations. Further research will be directed toward the improvement of the numerical performance of the proposed interfacing techniques. In this respect, main points of interest are: finding an accurate way to represent the ac network in the EMT part of the hybrid simulation without causing unrealistic controller reactions, exploring new methods to capture waveforms more accurately in the event of discontinuities, and finding generalizations with respect to arbitrary network arrangements.

## References

[1] P. Kundur, J. Paserba, V. Ajjarapu, G. Andersson, A. Bose, C. Canizares, N. Hatziargyriou, D. Hill, A. Stankovic, C. Taylor, T. Van Cursem, and V. Vittal, "Definition and classification of power system stability," *IEEE Transactions on Power Systems*, vol. 19, no. 3, pp. 1387–1401, 2004, cited By (since 1996): 137.

[2] B. Stott, "Power system dynamic response calculations," *Proceedings of the IEEE*, vol. 67, no. 2, pp. 219–241, Feb. 1979.

[3] J. Machowski, J. W. Bailek, and J. R. Bumby, *Power System Dynamics and Stability*. John Wiley & Sons, 1997.

[4] W. D. Humpage and B. Stott, "Predictor-corrector methods of numerical integration in digital-computer analyses of power-system transient stability," *Electrical Engineers, Proceedings of the Institution of*, vol. 112, no. 8, pp. 1557 –1565, august 1965.

[5] H. Dommel, "Digital computer solution of electromagnetic transients in single-and multiphase networks," *Power Apparatus and Systems, IEEE Transactions on*, vol. PAS-88, no. 4, pp. 388–399, April 1969.

[6] H. W. Dommel and W. S. Meyer, "Computation of electromagnetic transients," *Proceedings of the IEEE*, vol. 62, no. 7, pp. 983 – 993, July 1974.

[7] A.-R. Sana, J. Mahseredjian, X. Dai-Do, and H. Dommel, "Treatment of discontinuities in time-domain simulation of switched networks," *Mathematics and Computers in Simulation*, vol. 38, no. 4-6, pp. 377 – 387, 1995.

[8] M. Zou, J. Mahseredjian, G. Joos, B. Delourme, and L. Gérin-Lajoie, "Interpolation and reinitialization in time-domain simulation of power electronic circuits," *Electric Power Systems Research*, vol. 76, no. 8, pp. 688 – 694, 2006, selected Topics in Power System Transients.

[9] L. Harnefors, "Control of VSC-HVDC Transmission," tutorial presented at the IEEE Power Electronics Specialists Conference, Rhodos, Greece, Jun. 15–19 2008.

[10] V. Blasko and V. Kaura, "A new mathematical model and control of a three-phase AC-DC voltage source converter," *IEEE Transactions on Power Electronics*, vol. 12, no. 1, pp. 116–123, 1997.

[11] A. Gole, V. K. Sood, and L. Mootoosamy, "Validation and analysis of a grid control system using d-q-z transformation for static converter systems," in *Proc. Canadian Conf. on Electrical and Computer Engineering*, Montéal, CQ, Sep. 17–20, 1989.

[12] M. Heffernan, K. Turner, J. Arrillaga, and C. Arnold, "Computation of a.c.-d.c. system disturbances - parts I, II, and III. interactive coordination of generator and convertor transient models," *Power Apparatus and Systems, IEEE Transactions on*, vol. PAS-100, no. 11, pp. 4341 –4363, Nov. 1981.

[13] J. Reeve and R. Adapa, "A new approach to dynamic analysis of ac networks incorporating detailed modeling of dc systems - parts I and II," *Power Delivery, IEEE Transactions on*, vol. 3, no. 4, pp. 2005 –2019, Oct. 1988.

[14] M. Sultan, J. Reeve, and R. Adapa, "Combined transient and dynamic analysis of hvdc and facts systems," *Power Delivery, IEEE Transactions on*, vol. 13, no. 4, pp. 1271–1277, Oct 1998.

[15] V. Jalili-Marandi, V. Dinavahi, K. Strunz, J. A. Martinez, and A. Ramirez, "Interfacing techniques for transient stability and electromagnetic transient programs IEEE task force on interfacing techniques for simulation tools," *Power Delivery, IEEE Transactions on*, vol. 24, no. 4, pp. 2385–2395, Oct. 2009.

[16] K. Shintaku and K. Strunz, "Branch companion modeling for diverse simulation of electromagnetic and electromechanical transients," *Electric Power Systems Research*, vol. 77, no. 11, pp. 1501 – 1505, 2007.

[17] F. Gao and K. Strunz, "Frequency-adaptive power system modeling for multi-scale simulation of transients," in *Power and Energy Society General Meeting, 2010 IEEE*, Jul. 2010, p. 1.

[18] J. Arrillaga and N. R. Watson, *Computer Modelling of Electrical Power Systems*, 2nd ed. Chichester, UK: John Wiley & Sons LTD, 2002.

[19] T. Lobos, "Nonrecursive methods for real-time determination of basic waveforms of voltages and currents," *Generation, Transmission and Distribution, IEE Proceedings C*, vol. 136, no. 6, pp. 347 –352, Nov. 1989.

[20] A. A. van der Meer, R. L. Hendriks, and W. L. Kling, "Combined stability and electro-magnetic transients simulation od offshore wind power connected through multi-terminal VSC-HVDC," in *Proc. PES General Meeting*, Minneapolis, MN, Jul.19–24, 2010.


**Arjen van der Meer** obtained the B.Sc. degree at NHL University of applied sciences, Leeuwarden, the Netherlands, in 2006. In 2008, he received the M.Sc. degree from Delft University of Technology, the Netherlands.

Currently, he is working toward the Ph.D. degree at Delft University of Technology. His main research topic is the interconnection of large scale wind power to transnational offshore grids. His research interests include the modeling and simulation of renewable energy sources, power electronic devices, and protection systems.

**Ralph Hendriks** received the B.Sc. and M.Sc. degrees in electrical engineering from Delft University of Technology in 2003 and 2005 respectively.

Since 2005 he is a Ph.D. researcher at the High-Voltage Components and Power Systems group at Delft University of Technology, the Netherlands. His main research topic is grid integration of offshore wind farms through high-voltage direct current transmission, with a special focus on synergies with interconnectors. From 2007 he is also a consultant with Siemens AG, Erlangen, Germany.

His research interests include power system stability and control, grid integration of large-scale renewable energy sources and modeling of power electronics.

**Madeleine Gibescu** received her Dipl.Eng. in Power Engineering from the University Politehnica, Bucharest, Romania in 1993 and her MSEE and Ph.D. degrees from the University of Washington, Seattle, WA, U.S. in 1995 and 2003, respectively.

She has worked as a Research Engineer for ClearSight Systems, and as a Power Systems Engineer for the AREVA T&D Corp., U.S. She is currently an Assistant Professor with the Electrical Power Engineering department, Delft University of Technology, the Netherlands.

Her research interests include operations and planning for power systems with significant renewable energy penetration, with an emphasis on wind power.

**Wil Kling** received his M.Sc. degree in Electrical Engineering from the Eindhoven University of Technology, Eindhoven, the Netherlands, in 1978.

Since 1993, he has been a part-time Professor with the Delft University of Technology, the Netherlands in the field of Electrical Power Systems. Up till the end of 2008 he was also with TenneT, the Dutch Transmission System Operator, as senior engineer for network planning and strategy. Since Dec. 2008, he has been appointed Chair of the Electrical Power Systems group, Eindhoven University of Technology, the Netherlands. He is leading research programs on distributed generation, integration of wind power, network concepts and reliability issues.